ELSEVIER

Polymer 44 (2003) 167–176

polymer

www.elsevier.com/locate/polymer

A MALDI, TGA, TG/MS, and DEA study of the irradiation effects on PMMA

S.R. Tatro, G.R. Baker, K. Bisht, J.P. Harmon*

Department of Chemistry, University of South Florida, 4202 East Fowler Avenue, Tampa, FL 33620-5250, USA

Received 23 May 2002; received in revised form 30 September 2002; accepted 2 October 2002

Abstract

Poly(methyl methacrylate) (PMMA) ($M_w = 6.4 \times 10^3$, PD = 1.06) was irradiated under vacuum. The constant dose rate was 1.66×10^4 rad/min at doses between 10 and 100 Mrad using a cobalt-60 source. The samples were then analyzed by matrix assisted laser desorption/ionization (MALDI), hyphenated thermogravimetric/mass spectrometry (TG/MS), and dielectric analysis (DEA), all novel methods for the analysis of polymers damaged by radiation. Gel permeation chromatography (GPC), nuclear magnetic resonance (NMR), and differential scanning calorimetry (DSC) were also used for analysis. This study evidenced main chain scission, the removal of ester side groups, and the production of monomer as a result of ionizing radiation.

Keywords: Matrix assisted laser desorption/ionization; Poly(methyl methacrylate); Radiation

1. Introduction

This study focuses on the irradiation of highly syndiotactic poly(methyl methacrylate) (PMMA), and uses several novel methods to study radiation damage. By choosing a polymer that has been studied extensively [1–13], the results from the current study using novel techniques can be viewed in correlation with results of previously published findings.

It has been documented that when PMMA is exposed to both γ and ultraviolet radiation, main chain scission is the dominant occurrence in both air and vacuum [2,5]. As a result of the scission of the main chain, the molecular weight decreases, which, in turn, causes a decrease in the glass transition temperature [5]. Products include monomer, hydrogen gas, carbon dioxide, carbon monoxide, methane, and propane. The ratios of hydrogen, carbon dioxide, carbon monoxide, and methane to one another are roughly equivalent to the ratios of the elements contained in an ester side group [2].

A relatively new technique, matrix assisted laser desorption/ionization (MALDI), was developed in the late 1980s. The use of this technique allowed polymer molecules to be ionized and desorbed without fragmenting the molecules [14,15]. Its use for the analysis of synthetic polymers has been recently reviewed by McEwen and Peacock [16]. MALDI provides the weight average molecular weight (M_w), the number average molecular weight (M_n), and the polydispersity (PD). The classic definitions of these terms are as follows [17,18]

$$M_w = \frac{\sum N_x M_x^2}{\sum N_x M_x} \tag{1}$$

and

$$M_n = \frac{\sum N_x M_x}{\sum N_x} \tag{2}$$

where M_w is the weight average molecular weight, M_n is the number average molecular weight, N_x is the total number of molecules of length x, and M_x is the molecular weight of a molecule corresponding to a degree of polymerization x. The ratio of molecular weights is used to represent the breadth of the molecular weight distribution

$$PD = \frac{M_w}{M_n} \tag{3}$$

where PD is the polydispersity.

As research continued, studies demonstrated MALDI to be an optimum technique for polymers with a narrow molecular weight distribution while problems arise with

* Corresponding author. Tel.: +1-813-974-3397; fax: +1-813-974-1733.
E-mail address: harmon@chuma1.cas.usf.edu (J.P. Harmon).

0032-3861/03/$ - see front matter © 2002 Elsevier Science Ltd. All rights reserved.
PII: S0032-3861(02)00727-9

polydisperse polymers [19–25]. As a result of these findings, it must be concluded MALDI is a choice method for analyzing polymer standards [25], including standards used for the generation of Mark–Houwink–Sakurada parameters [26], and the PMMA standards used in this study. Previously, MALDI has been used to characterize biopolymers [16,27–29], synthetic polymers [19,30–32], and dendrimers [33,34], and to study the thermal degradation of PMMA [35]; however, no previous work has been done in which MALDI was used to study radiation damage of a polymer sample.

Another method of data collection, thermogravimetric analysis (TGA), involves the decomposition of a sample in order to characterize thermal stability [36]. TGA provides mass/temperature curves corresponding to mass changes as the polymer degrades [37] and has proven to be a very useful technique; however, information regarding the classification of the molecules responsible for the reduction in mass cannot be obtained through this system alone. In order to classify the compounds evolving from the decomposing polymer, thus greatly improving the system, some type of evolved gas analysis (EGA) can be used [37–42]. By coupling these two systems, both qualitative and quantitative information can be collected [37–39, 43–46]. There have been several TGA/EGA systems described in the literature. Some of these hyphenated systems include: TGA coupled with gas chromatography (GC), mass spectrometry (MS), or infrared spectroscopy (FTIR). Research has shown MS to be the most powerful and widely used [37,47,48]. The online coupling of these two procedures provides several advantages, which include speed and reduced sample handling [44]. Thermogravimetric analysis/mass spectrometry (TG/MS) has been available from several manufacturers since 1987 [37]. Past polymer studies (quantitative analysis, kinetics, analysis of evolved gases during synthesis, processing, and recycling, product development, reactivity and curing, structural characterization and chemical analysis, and thermal stability and degradation) have been previously reviewed [44].

Dielectric analysis (DEA) provides information about relaxations in polymers [49]. It has been previously documented that PMMA has three transitions. These transitions are labeled α, β, and γ, with decreasing temperature, and the α transition corresponds to the T_g [5, 50,51]. The β transition is associated with the rotation of the $-COOCH_3$ side group and can be observed through DEA of PMMA at low temperatures and low frequencies. At higher temperatures and frequencies, the β transition merges with the α transition resulting in an αβ transition corresponding to cooperative main chain slippage and side group rotation [52–55]. The γ transition is associated with rotation of the methyl groups attached directly to the main chain and can be observed in mechanical experiments. It cannot, however, be seen in dielectric experiments as the rotation of the methyl groups does not cause a change in the dipole moment of the polymer [56].

In DEA a sinusoidal voltage is applied to the sample causing polarization. By measuring the resulting current, the permittivity (ε') and the loss factor (ε''), which represent the amount of alignment of the dipoles and the energy required to align dipoles, respectively, can be determined. From this information, the tangent of the phase angle shift (tan δ can be calculated by Eq. (4) [57]

$$\tan \delta = \frac{\varepsilon''}{\varepsilon'} \tag{4}$$

The peak maximums in a tan δ vs. temperature plot can then be used to determine the α and β transition temperatures for several frequencies.

This is the first study combining the use of these techniques to study radiolysis of PMMA. These data were combined with data collected through gel permeation chromatography (GPC), nuclear magnetic resonance (NMR), and differential scanning calorimetry (DSC) to gain a more complete picture of what is occurring during the irradiation of PMMA.

2. Experimental

2.1. Materials

The PMMA standard was purchased from Polymer Source (Dorval, Canada). The PMMA standard was determined by Polymer Source to have a number average molecular weight of 6.4×10^3, a weight average molecular weight of 6.8×10^3, and a PD of 1.06 through size exclusion chromatography. The end groups of the PMMA, as determined by Polymer Source, consist of an isobutyl group and 2–3 α-methyl styrenes at the initiator end with a hydrogen at the terminal end. The tacticity, also determined by Polymer Source, is greater than 79% syndiotactic. The MALDI matrix, 3-β-indoleacrylic acid (IAA), and Cytochrome C calibration standard were purchased from Sigma (St. Louis, MO). Potassium chloride was purchased from J.T. Baker Chemical Corporation (Philipsburg, NJ). The solvents used were HPLC grade tetrahydrofuran (THF) purchased from Fisher Scientific (Pittsburgh, PA), and ethyl alcohol and chloroform-*d* ($CDCl_3$), purchased from Aldrich (Milwaukee, WI). The polymer standard was heated (100 °C) under a vacuum oven for several days to remove any residual solvent acquired during purification. All other materials were used without further purification.

2.2. Irradiation

The polymer samples were heated above the glass transition temperature to assist in oxygen removal and sealed under vacuum at a final pressure of 10^{-4} Torr. All samples (excluding the control) were irradiated at room temperature by gamma radiation from a ^{60}Co source. The constant dose rate was 1.66×10^4 rad/min at doses between

Table 1
MALDI data for irradiated and non-irradiated PMMA

Sample	M_n	M_w	PD	M_p
Control	7584	8009	1.06	7447
10 Mrad	6967	8097	1.16	7348
20 Mrad	5192	7165	1.38	7447
50 Mrad	4627	6735	1.46	7447
100 Mrad	3908	5589	1.53	7347

10 and 100 Mrad. After irradiation, samples were heated above the glass transition temperature (T_g) before vacuum was broken to annihilate free radicals.

2.3. MALDI sample preparation

The PMMA samples (1 mg) were dissolved in THF (1 ml). The matrix solution was prepared by dissolving IAA (20 mg) in THF (1 ml). In addition, a saturated solution of potassium chloride in ethanol was prepared. Polymer, matrix, and salt solutions were then mixed in a 10:40:4 μl, respectively. The samples (1–2 μl) were then spotted on the target and allowed to dry in the air. Once dry, the target was spotted again in the same fashion.

2.4. MALDI mass spectrometry

A Bruker REFLEX II MALDI-TOF instrument was used to obtain the mass spectrum data. The MALDI system includes the Scout source, High Mass detector®, delayed extraction, and XMASS data processing software [58]. A standard N_2 laser with a wavelength of 355 nm and a pulse width of 3 ns was used as the radiation source. The instrument was operated in the positive ion reflectron mode, and Cytochrome C was used as a calibration standard. The acceleration voltage and detector voltage were 25 and 1.5 kV, respectively. Each spectra is the sum of ~100 laser shots.

2.5. Gel permeation chromatography

Each sample was dissolved in THF and run on a Shimadzu LC-10AD Liquid Chromatograph with a flow rate of 1 ml/min. The GPC was equipped with both a RID-10A Refractive Index detector and a SPD-10AV UV–Vis detector with a wavelength of 254 nm, both of which are manufactured by Shimadzu.

2.6. Dielectric analysis

Dielectric data was collected using a TA Instruments 2970 DEA. The control and irradiated samples were heated (110 °C) under vacuum for several days after irradiation. This was done to remove any volatile compounds that could cause bubbling of the sample during analysis. The analysis was conducted under nitrogen purge from a temperature of −150 to 200 °C at a ramp rate of 5 °C/min. Single surface sensors were used as the samples were in powder form. A maximum force of 250 N was applied to the samples that reached a range of thickness from 0.3 to 1.4 mm. The loss factor (ε'') and tan δ were recorded at frequencies ranging from 10^{-1} to 3.0×10^8 Hz.

2.7. Differential scanning calorimetry

A TA Instruments 2920 DSC was used to determine the glass transition temperatures of the PMMA. Samples from 7 to 10 mg were scanned under a nitrogen purge at a ramp rate of 10 °C/min. Glass transition temperatures were determined on the second scan to assure identical thermal histories.

2.8. Thermogravimetric analysis/mass spectrometry

In order to conduct the TGA, 5–10 mg samples of PMMA were scanned using a TA Instruments HiRes TGA 2950. The data was obtained under a dry nitrogen purge using a Hi Res method and ramping at 20 °C/min from 50 to 475 °C. The TGA was coupled with a Pfeiffer Vacuum Thermostar GSD300T Mass Spectrometer.

2.9. Nuclear magnetic resonance

^{1}H NMR spectra were recorded using a Varian UNITY Plus 750 MHz NMR. ^{1}H NMR chemical shifts are reported downfield from 0.00 ppm using TMS as an internal standard. The concentrations were approximately 4% w/v in $CDCl_3$.

3. Results and discussion

3.1. MALDI

The changes in number average molecular weight (M_n), weight average molecular weight (M_w), PD, and the modal (M_p), most prevalent molecular weight, were all examined through the use of the MALDI for various radiation doses. As shown in Table 1 and as expected, there was a significant decrease in the M_n and M_w values as the total dose increases. The PD value increased noticeably with the increased dose indicating a larger distribution of chain lengths caused by main chain scission. While it is known that problems occur in samples with high polydispersities, these results are substantiated by the GPC data to be discussed in the following section. Fig. 1 is the MALDI spectra for each of the different doses. As the dose was increased, there was also an increase in the shorter chain length peaks. The most probable peak (M_p) value does not change at any dose suggesting the probability of chain scission being independent of chain length (refer to Table 1). In addition, the removal of the ester side group is noted by an increase in the

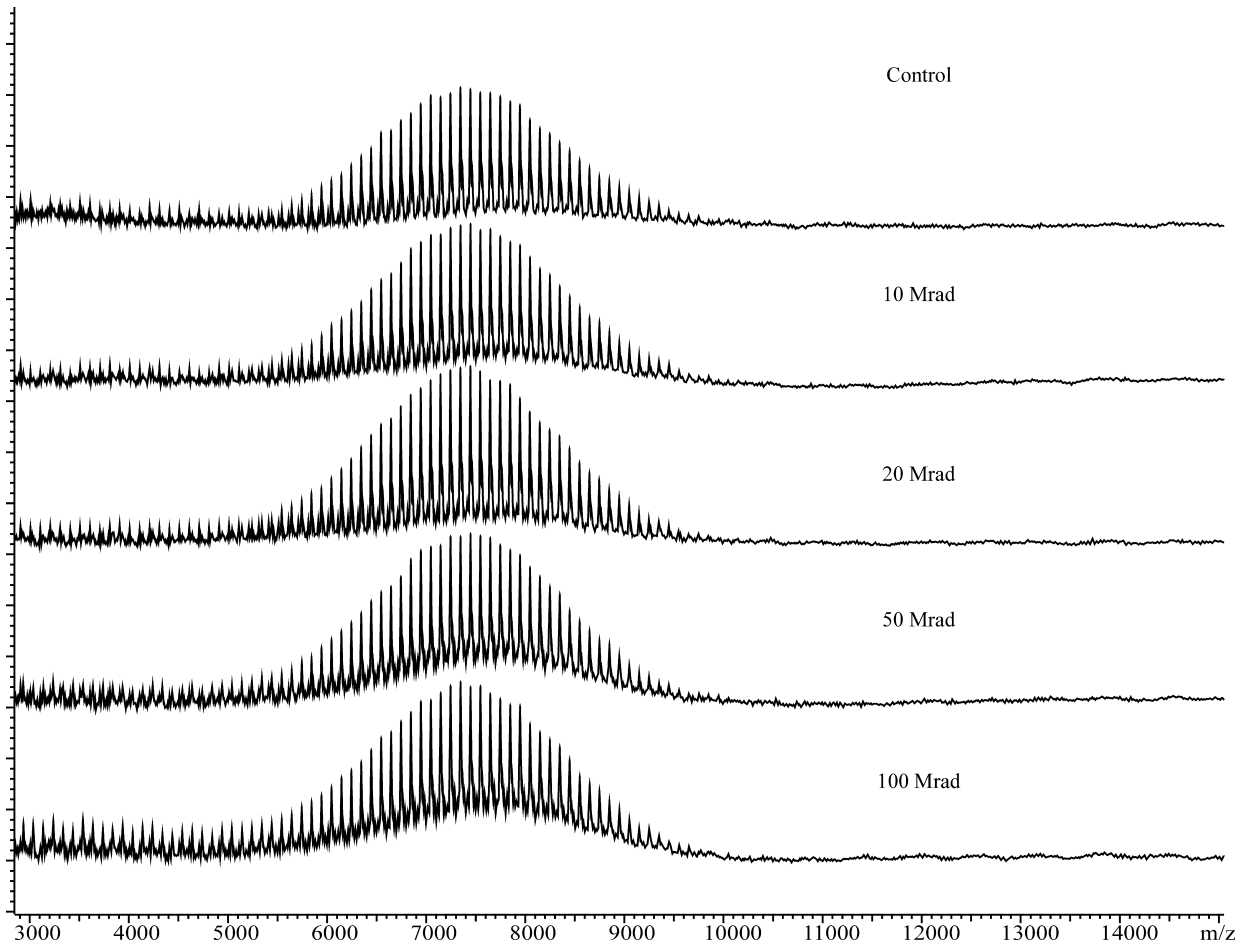

Fig. 1. MALDI molecular weight spectra for irradiated and non-irradiated PMMA.

peak corresponding to the loss of one side chain, which can be seen in Fig. 2. Peak A represents the intact polymer with two α-methyl styrene groups in the end group, and peak B corresponds to the intact polymer with three α-methyl styrene groups in the end group. Both are associated with a potassium ion. The mass to charge ratio (m/z) corresponding to peak C is 60 m/z less than the large peak of the intact polymer chain to the right (peak A), a value that is equivalent to the mass of one side group plus a hydrogen atom. This is consistent with a mechanism published by Guillet [59]. Table 2 provides the ratio of peak heights for peaks A and C (Fig. 2). Fig. 3 is a plot of the ratio of peak height vs. total dose. As seen in the plot, the ratio of peak heights is linearly related to the total dose.

Through the use of the MALDI, evidence for main chain scission was seen by the decrease in molecular weight and the increase in PD. The removal of one side group has also been clearly shown, suggesting the possibility of the polymer degradation beginning with the loss of the side group.

3.2. GPC

GPC was used to determine the changes in M_n, M_w, PD, and M_p. The GPC data in Table 3, data collected from the refractive index (RI) detector, and in Table 4, data collected from the ultraviolet (UV) detector, support the MALDI data by showing a decrease in the molecular weight and an increase in PD. The GPC data are, however, slightly lower than the MALDI data, and there is a slight decrease in M_p (Fig. 4). While the origin of the differences between the GPC and MALDI molecular weight data is unclear, the tendency for molecular weight data collected through MALDI to be slightly higher than that collected through GPC has been shown previously [20,24,25].

In the UV detector, a low molecular weight peak increases as the dose increases. This peak is not visible with the RI detector indicating the presence of a chromophore that absorbs at 254 nm with a refractive index similar to that of the solvent. The refractive index of THF is 1.407 [60] and the refractive index for methyl methacrylate is 1.414 as determined by Aldrich. These data suggest the low molecular weight peak illustrates the presence of monomer that increases with dose.

The GPC data shows agreement with the MALDI data, and therefore, substantiates the reliability of the data collected through the MALDI, including the decrease in molecular weight and the increase in PD.

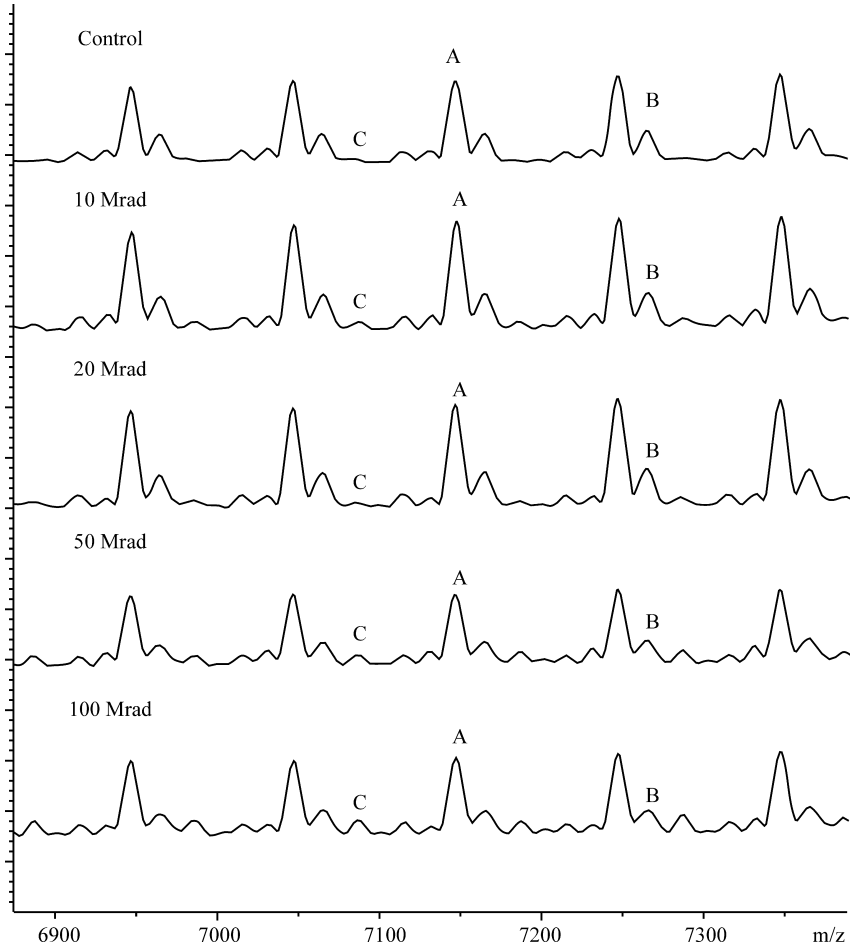

Fig. 2. MALDI molecular weight spectra for irradiated and non-irradiated PMMA, expanded view.

3.3. DEA

Because the MALDI data demonstrated the loss of a side group, the DEA was used for sample analysis to observe any possible changes in the β transition, the transition corresponding to the rotation of a side group. Over a wide range of frequencies, the loss factor (ε'') was measured at temperatures from −150 to 200 °C. (Fig. 5 is a representative DEA plot of ε'' vs. temperature.) Over the frequency range where the α and β transitions did not overlap, the natural log of the frequency was plotted vs. the inverse of the temperature at maximum peak height for the β peak giving a linear relationship indicating the β transition showed Arrhenius behavior. These plots were then used to calculate the activation energy (E_a) for the β transition. As seen in the DEA data presented in Table 5, E_a increases with the 10 Mrad sample and then steadily decreases with increasing doses. The E_a of the β transition for the control group (17.7 kcal/mol) agreed with the E_a for neat atactic PMMA (17.6 kcal/mol) published by Emran et al. [34], and the decrease in E_a with increased dose can be attributed to

Table 2
MALDI data for irradiated and non-irradiated PMMA: ratio of peak heights. Peak C: polymer chain after the removal of one side group. Peak A: intact polymer chain

Sample	Peak C/peak A
Control	0.014
10 Mrad	0.043
20 Mrad	0.075
50 Mrad	0.144
100 Mrad	0.214

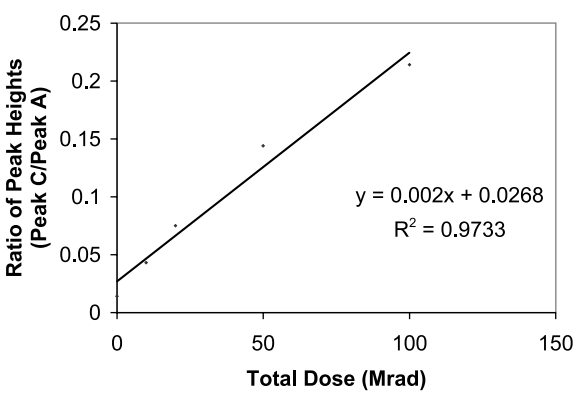

Fig. 3. Ratio of peak heights determined from MALDI vs. total dose.

Table 3
GPC Data for irradiated and non-irradiated PMMA: refractive index detector

Sample	M_n	M_w	PD	M_p
Control	5488	5889	1.073	5995
10 Mrad	5144	5698	1.108	5995
20 Mrad	5022	5684	1.132	5995
50 Mrad	5678	5227	1.421	5819
100 Mrad	2152	4329	2.012	5647

Table 4
GPC Data for irradiated and non-irradiated PMMA: ultraviolet detector

Sample	M_n	M_w	PD	M_p
Control	5368	5850	1.090	6048
10 Mrad	4583	5483	1.196	5871
20 Mrad	4155	5229	1.258	5871
50 Mrad	3389	4693	1.385	5699
100 Mrad	2928	4180	1.428	5369

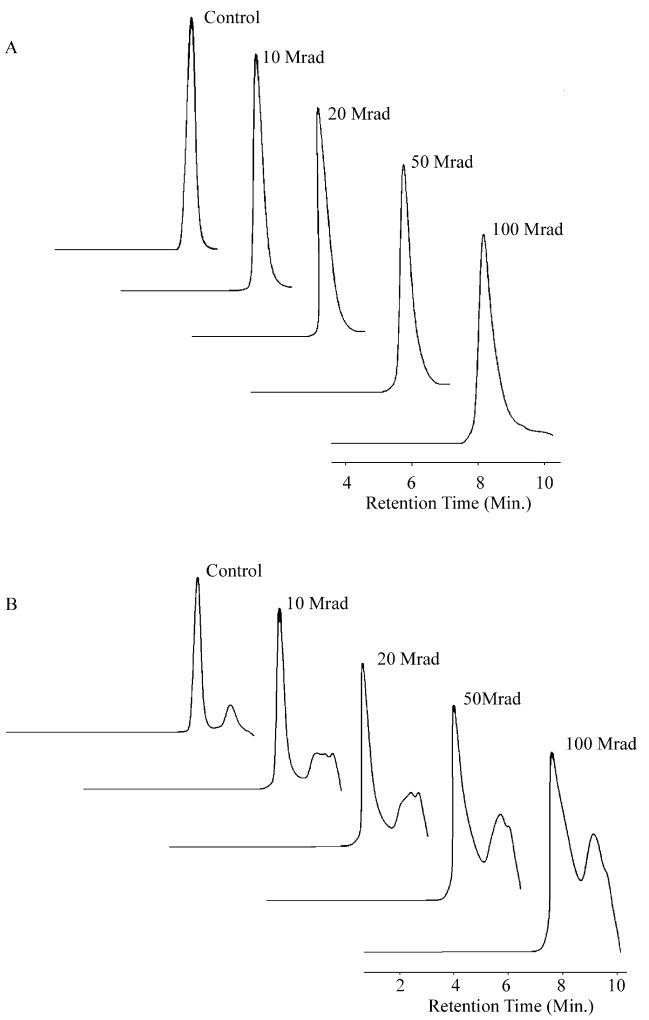

Fig. 4. GPC data for irradiated and non-irradiated PMMA, (A) refractive index detector, (B) ultraviolet detector.

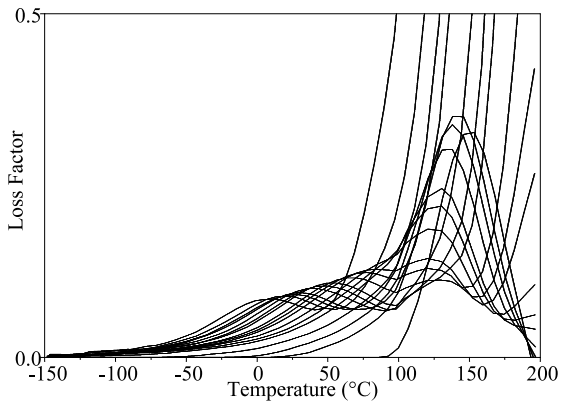

Fig. 5. Representative DEA plot for PMMA. Plot shown is 20 Mrad sample.

scission increasing the free volume, which, in turn, enhances the ease of motion.

The Williams, Landel, and Ferry (WLF) equation [56]

$$\ln a_T = \frac{-C_1(T - T_0)}{C_2 + (T - T_0)} \quad (5)$$

where a_T is the shift factor which corresponds to frequency, T_0 is a reference temperature which corresponds to T_g, T is a given temperature, and C_1 and C_2 are WLF constants [61], is often applicable to the α transition of amorphous polymers [56]; however, this relationship could not be applied as a result of extensive merging of the α and β relaxations.

For one of the few frequencies in which there was separation of the α and β transitions, tan δ was used to determine the degree of separation and the ratio of peak heights. Data collected at 100 Hz is shown in Table 6. Syndiotactic PMMA shows two separate α and β transitions at lower frequencies, the β transition being the dominant of the two, while for isotactic PMMA the transitions are partially merged with the α transition being the dominant of the two transitions [56]. The degree of separation between

Table 5
DEA data for irradiated and non-irradiated PMMA: Arrhenius β transition

Sample	E_a (kcal/mol)
Control	17.7
10Mrad	19.7
20 Mrad	18.6
50 Mrad	18.4
100 Mrad	15.1

Table 6
Dielectric data for α and β relaxations of irradiated and non-irradiated PMMA at 100 Hz

Sample	T_α (°C)	tan δ_α	T_β (°C)	tan δ_β	tan δ_α/tan δ_β	$T_\alpha - T_\beta$ (°C)
Control	122	0.028	50	0.049	0.57	72
10 Mrad	120	0.042	49	0.074	0.57	71
20 Mrad	122	0.037	50	0.050	0.74	72
50 Mrad	114	0.041	54	0.043	0.95	60
100 Mrad	116	0.081	54	0.062	1.3	62

Table 7
DSC data for irradiated and non-irradiated PMMA

Sample	T_g (°C)	Breadth of transition (°C)
Control	119.32	9.31
10 Mrad	116.83	10.21
20 Mrad	112.71	11.77
50 Mrad	104.97	14.28
100 Mrad	95.24	15.55

the α and β transitions for the irradiated samples remained relatively constant up through 20 Mrad (Table 6). At 50 Mrad, the degree of separation drops significantly and then once again remains constant. The decrease in separation was due to a decrease in T_g caused by scission.

The ratio of peak heights (Table 6), tan δ_α/tan δ_β evidences a trend. The ratio remains constant through 10 Mrad and then increases at the dose increases illustrating the emergence of the α transition as the dominant peak, a result of the loss of the ester side groups.

This study will be expanded to include further tacticities to determine if the same trends are evident as configuration has a significant effect on the peak height ratios and the separation of the two transitions.

3.4. DSC

DSC was used to examine the change in the T_g cause by exposure to irradiation. Table 7 shows the T_g and breadth of transition for various doses of radiation. As the radiation dose increases, the T_g of the PMMA decreases. The decrease in T_g is a result of the decrease in molecular weight already demonstrated by MALDI. In addition to the decrease in molecular weight, there is also an increase in the breadth of the transition. The breadth of the transition starts at 9.31 °C for the control group and increases to 15.55 °C for the 100 Mrad sample, a change of 67%. A completely homogenous material demonstrates a very narrow transition breadth, and a broad transition indicates a heterogeneous blend [62]. Thus, the increase in the breadth of the transition evidences an increase in the content of radiation products, including monomer, as the total dose is increased.

Fig. 6 shows the linear relationship between the total dose and the T_g. The T_g vs. dose is plotted to give an R^2 value of 0.9868. In Fig. 7, the T_g vs. $1/M_n$ is also plotted using M_n values obtained by MALDI and M_n values obtained by GPC. The linear relationship is obvious for the MALDI data, giving an R^2 value of 0.9467, while the GPC data is somewhat scattered, giving an R^2 value of only 0.6608.

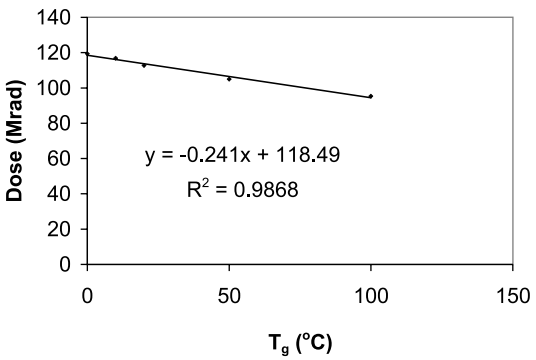

Fig. 6. Glass transition temperature determined by DSC vs. total dose.

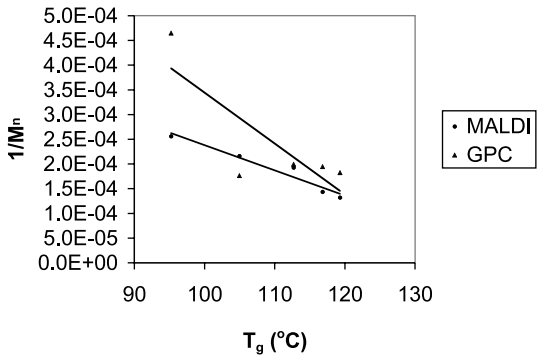

Fig. 7. Glass transition temperature determined by DSC vs. molecular weight data determined by MALDI and GPC.

The decrease in the T_g demonstrates the decrease in molecular weight, supporting MALDI and GPC, and is linearly related to the total dose.

3.5. TGA

As the molecular weight decreases, the thermal stability of the polymer should also decrease [62]. Table 8 presents the decomposition temperature for the different radiation doses. The degradation temperature remains constant until a dose of 50 Mrad is delivered, at which point there is a significant drop. As the dose is increased further to 100 Mrad, the degradation temperature once again remains relatively constant. Fig. 8 plots the derivative of the weight loss vs. the temperature for the different radiation doses. The increase in the broadness and the earlier onset of the peak with increased dose suggest the possibility of an increase in the amount of monomer in the sample and an increase in PD. The decrease in molecular weight and increases in PD support the previously stated conclusions.

3.6. TG/MS

The data showing the decrease in temperature of degradation for the samples can be enhanced by the use of

Table 8
HiRes TGA data for irradiated and non-irradiated PMMA

Sample	Decomposition temperature (°C)
Control	336
10 Mrad	336
20 Mrad	334
50 Mrad	322
100 Mrad	326

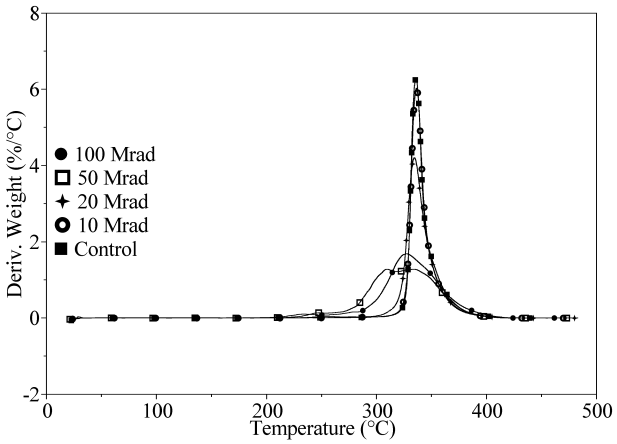

Fig. 8. HiRes TGA data for irradiated and non-irradiated PMMA.

TG/MS. The abundance of the *m*/*z* 41, 69, and 100 signals vs. temperature can be seen in Fig. 9. These are the most abundant ions seen in the mass spectrum of methyl methacrylate [63]. The *m*/*z* 100 signal corresponds to the entire monomer, the *m*/*z* 69 signal corresponds to the monomer after the loss of $-OCH_3$ from the side chain, and the *m*/*z* 41 signal corresponds to the monomer after the loss of the entire side chain ($-COOCH_3$). For the control group, as the temperature increases there is a steady increase in the abundance of these peaks. As the radiation dose is increased, a separate peak around 240 °C emerges until it can be clearly seen in the 100 Mrad sample. This peak evidences the presence of monomer in the sample. These TG/MS data support the conclusion that the amount of monomer in the sample increases and thermal stability decreases with increased total radiation dose.

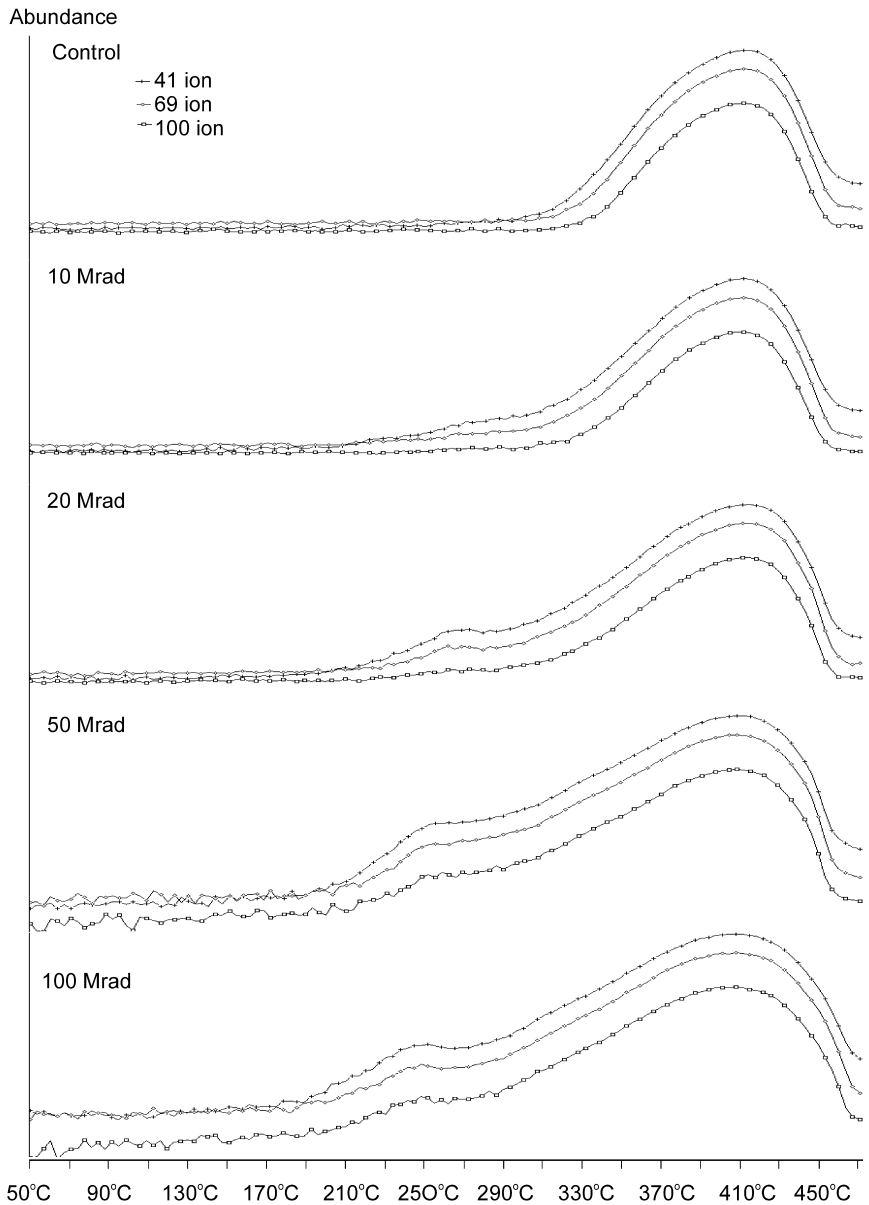

Fig. 9. TG/MS data for irradiated and non-irradiated PMMA.

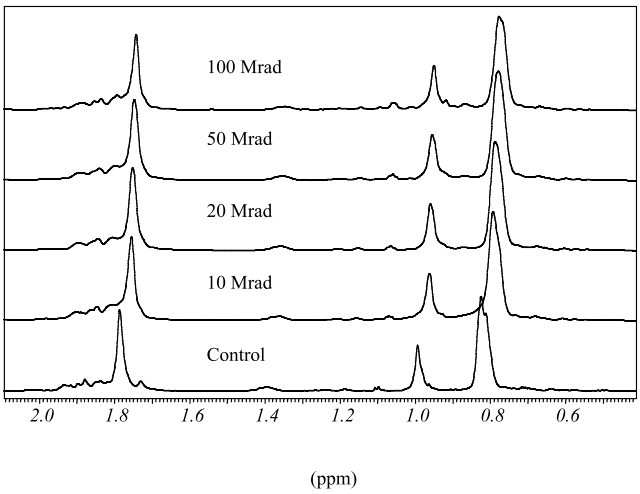

Fig. 10. ^{1}H NMR data for irradiated and non-irradiated PMMA.

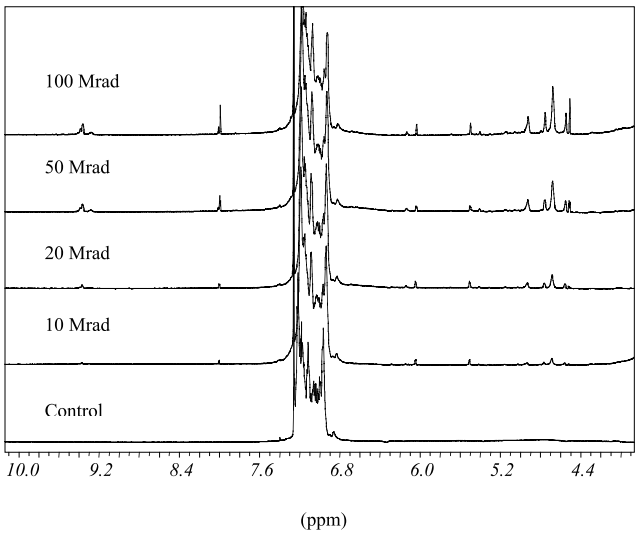

Fig. 11. ^{1}H NMR data for irradiated and non-irradiated PMMA.

3.7. NMR

In order to substantiate the previously stated conclusion regarding an increase in monomer content corresponding to an increase in radiation dose, NMR was used. Figs. 10 and 11 show the ^{1}H NMR spectra for PMMA. The signals in the 0.7–1.2 ppm range indicate the polymer sample is highly syndiotactic, as the dominant signal in the 0.7–0.8 ppm range corresponds to the syndiotactic content of the polymer, the signal in the 0.9–1.0 ppm range corresponds to the atactic content of the polymer, and the signal in the 1.1 ppm range corresponds to the isotactic content of the polymer [64]. These signals can be assigned to the α-methyl hydrogens, and the lack of change in their peak height ratios indicates there was no significant change in tacticity. The signal in the 1.8 range can be assigned to the hydrogens in the polymer backbone ($-CH_2-$) (Fig. 10) [65]. When looking at Fig. 10, there appears to be an upfield shift and a decrease in resolution as the dose is increased.

In Fig. 11, the signals centered around 7.1 ppm can be attributed to the α-methyl styrene end groups [66]. Also in Fig. 11, there is the emergence of several small peaks as the dose is increased. The signals in the 4.3–5.0 ppm range can be attributed to unsaturation of the polymer chain ends and backbone and the formation of dimethoxy methane ($-CH_2-$ group) [64]. The signals at 6.1 and 5.5 ppm are indicative of the presence of monomer in the sample [2,66], as previously stated. Although, to the knowledge of the authors, this has not been previously reported, the signal at 8.0 ppm suggest the possisbility of formic acid in the sample, and the signal at 9.3 ppm evidences the presence of methacrylaldehyde in the sample [65]. All of these signals show an increase as dose is increased.

This ^{1}H NMR data supports the previously made conclusion regarding an increase in the presence of monomer in the sample as the dose is increased. It also indicates unsaturation of the backbone and chain ends and the possible production of formic acid, dimethoxy methane, and methacrylaldehyde.

4. Conclusion

The irradiation of PMMA under vacuum was investigated through the use of MALDI, GPC, DEA, DSC, TGA, TG/MS, and NMR. The MALDI data demonstrated a decrease in M_w and M_n and an increase in PD, which was supported by the GPC data; however, MALDI was able to show the removal of a side group from an otherwise intact polymer chain, which could not be seen with GPC. Thus, indicating that MALDI is a valuable tool in observing the structural changes in irradiated polymers.

For the first time, DEA was used to show the dominant transition shift from the β relaxation to the α relaxation evidencing the removal of the ester side groups as a result of irradation.

The combination of TGA with MS also proved to be a valuable resource. Through the linkage of these two methods, a clear picture of the monomer contained in the irradiated samples can be seen by the emergence of the peak at 240 °C in the mass spectra of the irradiated samples. This substantiates the data obtained from GPC and NMR.

When PMMA is irradiated, with increasing radiation doses, main chain scission occurs, a side group is removed first, and monomer is produced, all of which have been known to occur for many years now; however, this is the first study in which these novel techniques have been used for this purpose. The data obtained through these techniques showed agreement with previous findings, thus developing a new method to study the radiation effects on polymeric materials.

Acknowledgements

The authors would like to thank Talal Al-Azemi for his help with the NMR and GPC data, Dr Katherine Williams of the University of Florida for her help for the use of the irradiation chamber, Dr Charles Moorefield and Dr Venkat R. Dudipala of the University of Akron for their help with the NMR data, and Dr Michael Zaworotko for the use of the TG/MS.

References

[1] Kudoh H, Sasuga T, Seguchi T, Katsumura Y. Polymer 1996;37(21): 4663–5.
[2] Reich L, Stivala S. Elements of polymer degradation. New York: McGraw-Hill; 1971. Chapter 1.
[3] Shrempel F, Witthuhn W. Nuclear Instrum Meth Phys Res B 1997; 132:430–8.
[4] Ichikawa T, Oyama K, Kondoh T, Yoshida H. J Polym Sci, Part A: Polym Chem 1994;32:2487–92.
[5] Goyanes SN, Benites GM, González JJ, Rubiolo GH, Marzocca AJ. Polym Test 1997;16:7–18.
[6] Okudaira KK, Morikawa E, Hasegawa S, Sprunger PT, Saile V, Seki K, Harada Y, Ueno N. J Electron Spectrosc 1998;88–89:913–7.
[7] Goyanes SN, Benites GM, Rubiolo GH, Marzocca AJ. J Phys III 1996;6:587–90.
[8] Sayyah SM, Sabbah IA, Ayaub MMH, Barsoum BN, Elwy E. Polym Degrad Stab 1997;58:1–9.
[9] El-Salmawi K, Abu Zeid MM, El-Naggar AM, Mamdouh M. J Appl Polym Sci 1999;72:509–20.
[10] Gaynor J, Schueneman G, Schuman P, Harmon JP. J Appl Polym Sci 1993;50:1645–53.
[11] Harmon JP, Gaynor JF, Taylor AG. Radiat Phys Chem 1993;41: 153–64.
[12] Bertolucci PRH, Harmon JP. Polym Engng Sci 1998;38:699–705.
[13] Harmon JP, Gaynor JF. J Polym Sci, Part B: Polym Phys 1993;31: 235–6.
[14] Karas M, Hillenkamp F. Anal Chem 1988;60:2299–301.
[15] Hillenkamp F, Karas M, Beavis RC, Chait BT. Anal Chem 1991;63: 1193–203.
[16] McEwen CN, Peacock PM. Anal Chem 2002;74:2743–8.
[17] Campbell I. Introduction to synthetic polymers. Oxford: Oxford University Press; 1994. p. 45, see also p. 18–9.
[18] Stevens M. Polymer chemistry, 3rd ed. New York: Oxford University Press; 1999. p. 168.
[19] Larsen BS, Simonsick Jr. WJ, McEwen CN. J Am Soc Mass Spectrosc. 1996;7:287–92.
[20] Thompson B, Suddaby K, Rudin A, Lajoie G. Eur Polym 1996;32(2): 239–56.
[21] Lehrle RS, Sarson DS. Polym Degrad Stab 1996;51:197–204.
[22] Guo B, Chen H, Rashidzadeh H, Liu X. Rapid Commun Mass Spectrom. 1997;11:781–5.
[23] Danis PO, Karr DE, Simonsick Jr. WJ, Wu DT. Macromolecules 1995;28:1229–32.
[24] Cottrell JS, Koerner M, Gerhards R. Rapid Commun Mass Spectrom. 1995;9:1562–4.
[25] Zhu H, Yalcin T, Li L. J Am Soc Mass Spectrosc 1998;9:275–81.
[26] Tatro SR, Baker GR, Fleming R, Harmon JP. Polymer 2002;43: 2329–35.
[27] Karas M, Bahr U, Geissman U. Mass Spectrom Rev 1992;10:335–7.
[28] Beavis RC, Chait BT. Rapid Commun Mass Spectrom 1989;3:432–5.
[29] Spengler B, Pan Y, Cotter RJ, Kan LS. Rapid Commun Mass Spectrom 1990;4:99–102.
[30] Jackson AT, Bunn A, Hutchings LR, Kiff FT, Richards RW, Williams J, Green MR, Bateman RH. Polymer 2000;41:7437–50.
[31] Montaudo G, Garozzo D, Montaudo M, Puglisi C, Samperi F. Macromolecules 1995;28:7983–9.
[32] Hanton SD. Chem Rev 2001;101:527–69.
[33] Emran SK, Newkome GR, Weis CD, Harmon JP. J Polym Sci, Part B: Polym Phys 1999;37:2025–38.
[34] Emran SK, Liu Y, Newkome GR, Harmon JP. J Polym Sci, Part B: Polym Phys 2001;39:1381–93.
[35] Borman CD, Jackson AT, Bunn A, Cutter AL, Irvine DJ. Polymer 2000;41:6015–20.
[36] Kaisersberger E, Post E. Thermochim Acta 1998;324:197–201.
[37] Groenewoud WM, Jong W. Thermochim Acta 1996;286:341–54.
[38] Statheropoulos M, Kyriakou S, Tzamtzis N. Thermochim Acta 1998; 322:167–73.
[39] Szelely G, Nebuloni M, Zerilli LF. Thermochim Acta 1992;196: 511–32.
[40] Leskelä T, Lippmaa M, Niinistö L, Soininen P. Thermochim Acta 1993;214:9–18.
[41] Holdiness MR. Thermochim Acta 1984;75:361–99.
[42] Dollimore D, Gamlen GA, Taylor TJ. Thermochim Acta 1984;75: 59–69.
[43] Jaenicke-Röβler K, Leitner G. Thermochim Acta 1997;295:133–45.
[44] Raemaekers KGH, Bart JC. Thermochim Acta 1997;295:1–58.
[45] Mittleman M. Thermochim Acta 1990;166:301–8.
[46] Maciejewski M, Bailer A. Thermochim Acta 1997;295:95–105.
[47] Jansen JAJ, Haas W. Anal Chim Acta 1987;196:69–74.
[48] Redfern JP. Polym Int 1991;26:51–8.
[49] Gedde UW. Polymer physics. London: Chapman & Hall; 1995.
[50] Roberts GE, White EFT. The physics of glassy polymers. London: Applied Science Publishers; 1973. p. 153.
[51] Heijboer J. Molecular basis of transitions and relaxations. London: Meier/Gordon and Breach; 1978. p. 75.
[52] Calves MC, Harmon JP, ACS Symposium Series, Washington, DC: American Chemical Society; 2001.
[53] Harmon JP, Noren GK. Optical polymers: fibers and waveguides. Washington, DC: American Chemical Society; 2001. chapter 6.
[54] Aihara T, Saito H, Inoue T, Wolff HP, Stühn B. Polymer 1998;39(1): 129–34.
[55] Higgenbotham-Bertolucci PR, Gao H, Harmon JP. Polym Engng Sci 2001;41:873–80.
[56] McCrum NG, Read BE, Williams G. Anelastic and dielectric effects in polymeric solids. New York: Dover Publications; 1967.
[57] TA Instruments. DEA 2970 Dielectric Analyzer Operator's Manual 1991.
[58] XMASS data processing software, version 3.1. Bruker; May 1997.
[59] Guillet J. Polymer photophysics and photochemistry. Cambridge: Cambridge University; 1985.
[60] The Merck Index. 12th ed. Whitehouse Station: Merck Research Laboratories; 1996.
[61] Emran SK. Doctoral Dissertation. Viscoelastic properties of dendrimers, dendrimer blends, and dendrimer gels. Florida: 2000.
[62] Turi EA. Thermal characterization of polymeric materials. New York: Academic Press; 1981.
[63] National Institute of Standards and Technology. Chemistry WebBook. webbook.nist.gov/chemistry/2002.
[64] Dong L, Hill D, O'Donnell J, Carswell-Pomerantz T, Pomery P, Whittaker A, Hatada K. Macromolecules 1995;28:3681–91.
[65] Subramanian K. Eur Polym J 2001;37:55–64.
[66] Pouchert CJ. The Aldrich library of NMR spectra. Milwaukee: Aldrich Chemical Company, Inc.; 1983.